Spatial and temporal features in microwave and ultraviolet emission for eruptive and confined events

I.A. Bakunina[1], V.F. Melnikov[2], V.E. Abramov-Maximov[2], A.S. Morgachev[3], A.V. Shain[2]

[1]*National Research University Higher School of Economics, Nizhny Novgorod, Russia*

[2]*Pulkovo Observatory, St.Petersburg, Russia*

[3]*Lobachevsky State University, Nizhniy Novgorod, Russia*

ESPM-16

Solar flares and coronal mass ejections (CME) are the most powerful manifestations of solar activity. Both phenomena associated with the evolution of the spatial structure of the magnetic field of active regions (ARs). It is known that not all powerful flares accompanied by CME. In some cases, CME are observed, associated with very low intensity bursts. At the same time the observational signs that determine the ability of AR to cause the eruption of matter from AR into the high layers of the solar corona are still not clear. This makes it difficult for us to understand the eruption initiation physical mechanism (CME trigger). The purpose of this work is to search for observational signs of the onset of eruptive process. For this, we conducted a comparative analysis of pre-flare and flare conditions for flare events, accompanied by CME, and events not accompanied by CME. We studied the features of the spatial dynamics of the microwave and ultraviolet emission (data from the Nobeyama Radioheliograph and SDO/AIA) of AR for selected events.

We will call flares which are not accompanied by CMEs «confined» and flares with CME «eruptive».

Observations of active regions (ARs)

In our study, we examined the behavior of microwave and ultraviolet emission of active regions in the interval of several hours before X-ray class M flares.

The analysis was carried out on the basis of radio maps of the Sun obtained with the Nobeyama radioheliograph at a frequency of 17 GHz with a two-dimensional spatial resolution of 10 "- 15", with a time interval between images of 3 minute and an averaging time of 10 seconds, and on the basis of SDO/AIA observational data in the EUV (extreme ultraviolet) range 94A and 131A with ~ 1.5 ” spatial resolution.

We analyzed 11 flares that were selected from (Duan et al., 2019). The sample included only those events, the observation time of which fell within the observation interval of the Nobeyama Radioheliograph (22:50 - 06:20 UT).

Table 1

Date	Flare peak time	Flare class	NOAA	Flare position	E/C	NoRH F17 (SFU)	Tb (K)	Dur (sec)	The square of radio source (angular sec^2)
2011-07-30	02:09	M9.3	11261	N16E19	C	569	5.8e+07	594	15000
2011-10-02	00:50	M3.9	11305	N09W12	C	42	2.2e+06	4149	12500
2012-05-10	04:18	M5.7	11476	N13E22	C	54	5.2e+06	363	18750
2013-11-03	05:22	M5.0	11884	S12W16	C	233	1.3e+07	4203	18750
2014-02-04	04:00	M5.2	11967	S14W06	C	3572	3.0e+07	1556	22500
2011-09-06	01:50	M5.3	11283	N14W07	E	206	2.0e+07	3770	39375
2012-01-23	03:59	M8.7	11402	N28W21	E	3703	7.4e+07	16207	60000
2012-03-09	03:53	M6.3	11429	N15W03	E	90	3.9e+06	4986	45000
2013-10-24	00:28	M9.3	11877	S10E08	E	78	2.9e+06	1042	33750
*2014-09-28	02:58	M5.1	12173	S13W23	E	373	2.0e+06	3118	30000
2014-12-17	04:42	M8.7	12242	S20E09	E	236	8.0e+06	8808	30000

E – eruptive, C – confined

6 flares accompanied by CME, and 5 - unaccompanied by CME ("confined")

In both samples of events “E” (eruptive) and “C” (confined), only M-class flares are present. It is clear from the last four columns of Table 1 that, for the selected four parameters of radio emission for class M flares, there are mainly no events with a higher flux, brightness temperature, or flare duration for the “E” or “C” sample.
The differences are manifested only in the size of radio sources: as can be seen from the far right column of Table 1, events with CME demonstrate radio sources that are more extensive in area.

Earlier in our works (Bakunina and Melnikov, 2019; Bakunina et al., 2020 a; Bakunina et al., 2020 b), the phenomenon of strong nonstationarity of microwave sources was discovered, associated with the appearance 1– 3 or more hours before the flare of intersecting bright and "hot" ($T \sim 10^7$ K) ultraviolet loops.

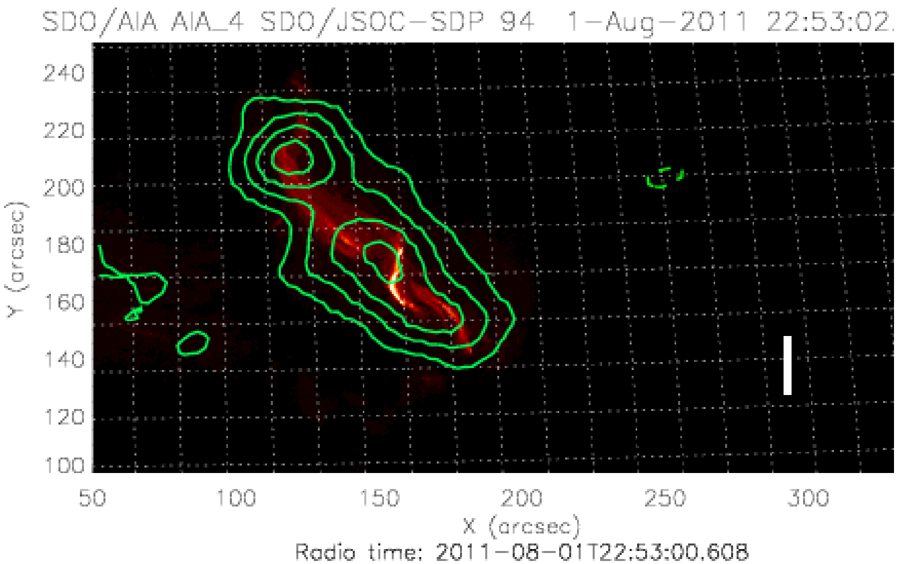

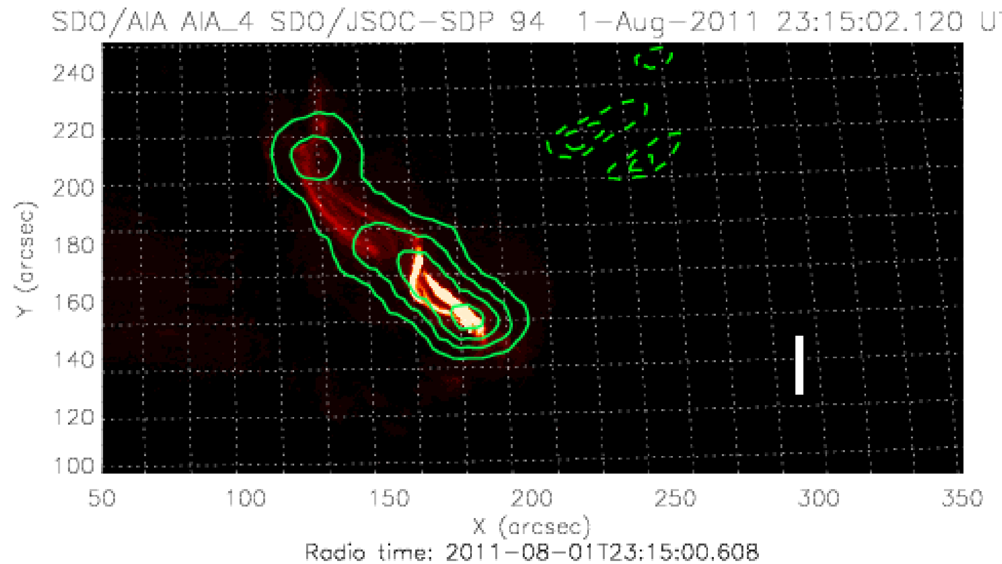

6.5 hours before the flare of M 1.4 (05:19) in the ultraviolet range (94 A), a system of bright intersecting loops is visible, which persists until the onset of the flare.

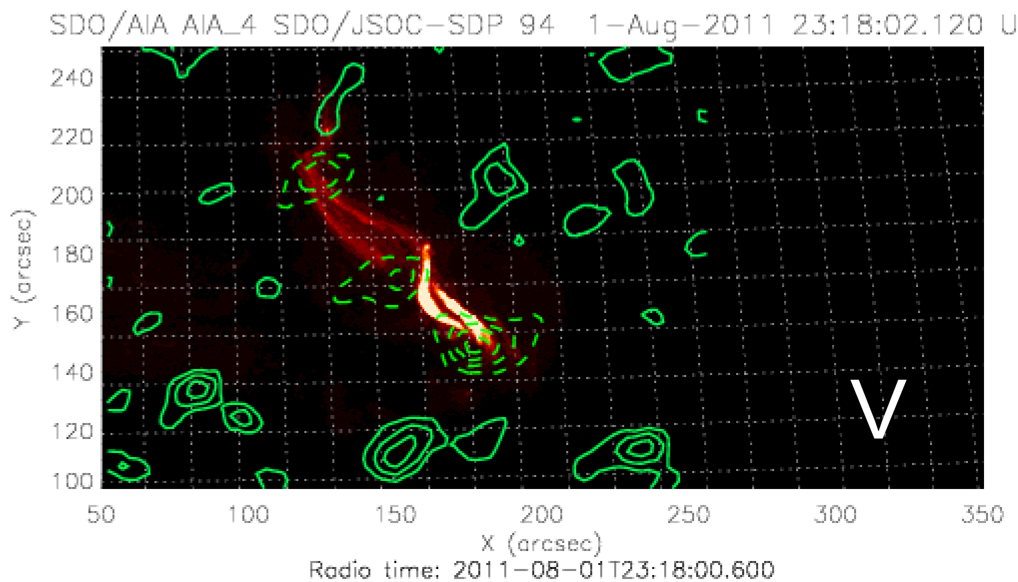

AR 11261, 02082011

It is at the location of this transverse EUV (extreme ultraviolet) loop the M1.4 flare begins.

In the radio range, a source with different signs of polarization at the site of the transverse EUV loop appears during the first phase of the flare.

(contours - polarization,17 GHz)

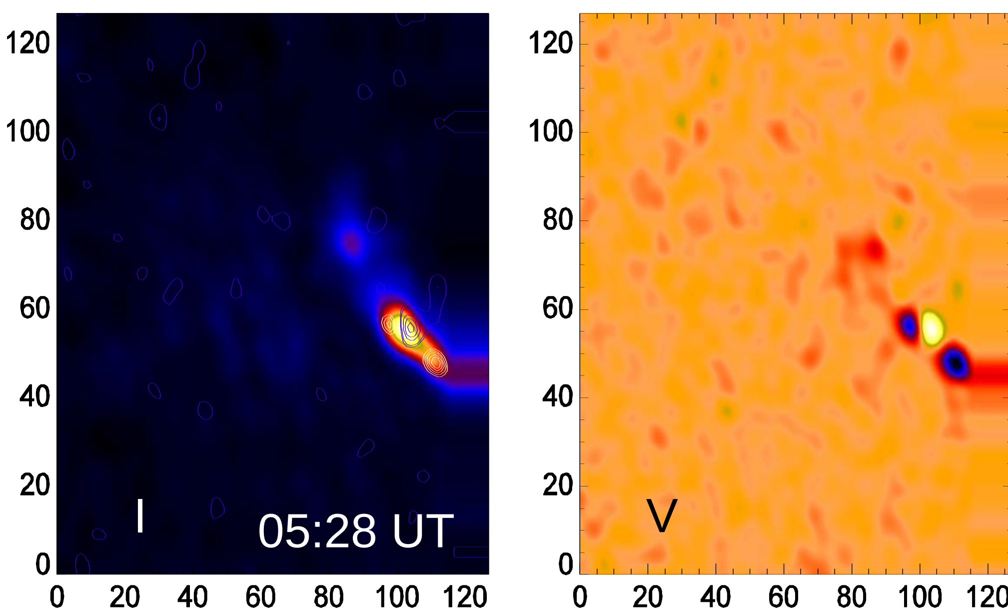

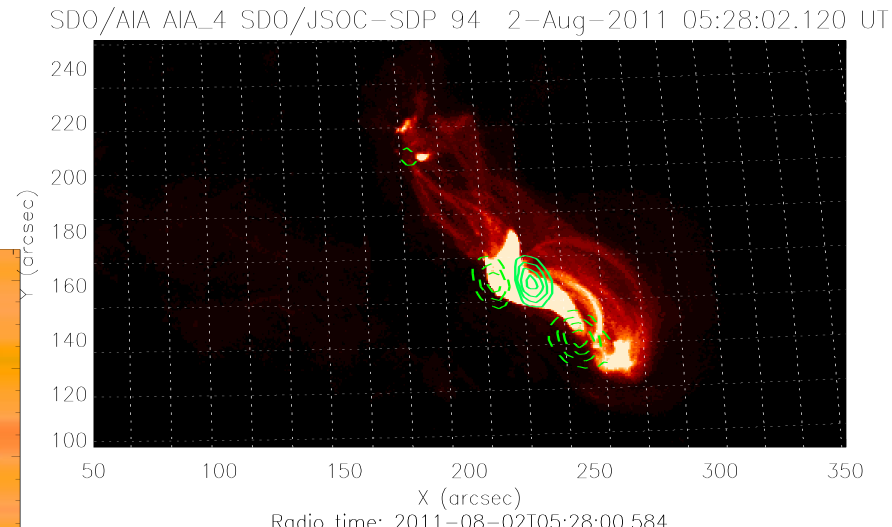

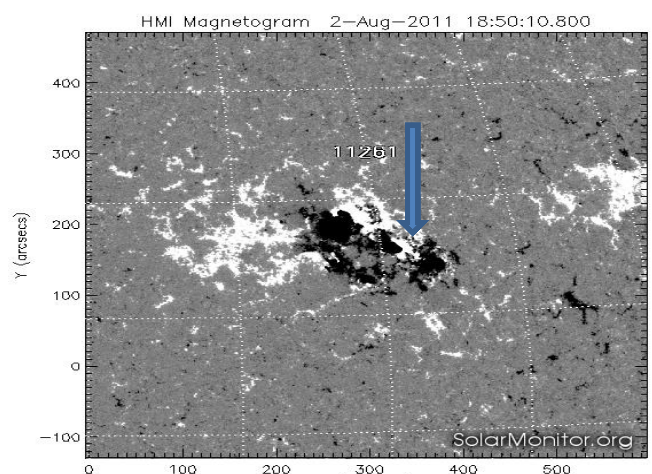

Fine spatial structure of sources

Plasma heated to very high temperatures ~ 10 ^ 7 K is responsible for EUV radiation in the 94 A line. The fact that bright loops in this line are visible for hours in AR indicates the presence of hot, T = 10 million K, plasma in them. This means that energy is released for hours in the AR.

A bright EUV loop has appeared(at 01:42 UT) –
a precursor of the appearance of a new horizontal structure of the microwave source

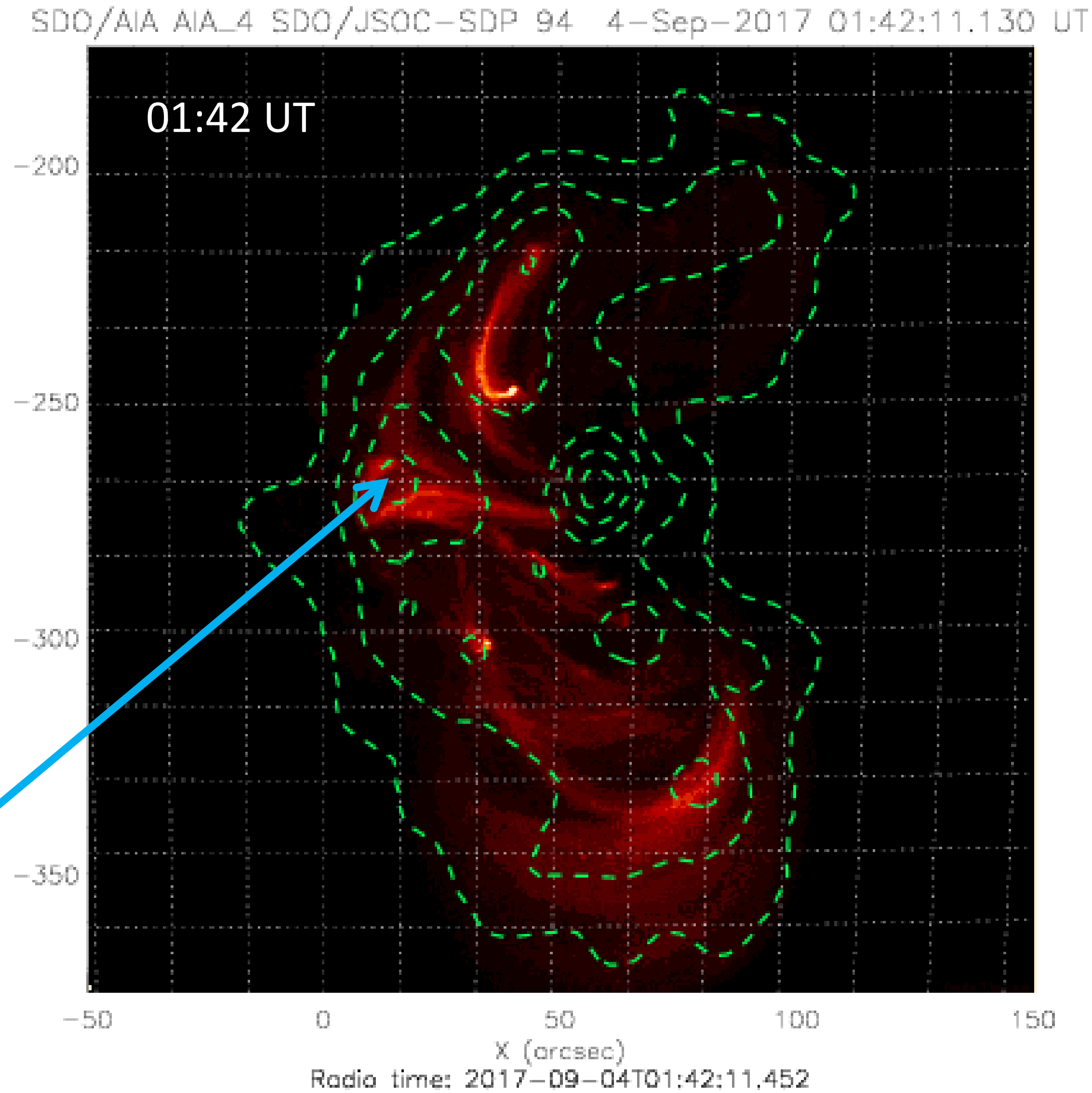

AR 12673

Observations on the Nobeyama Radioheliograph, September 4, 2017

Dynamics of the spatial structure of a radio source before flare M1.2 (05:36 UT)

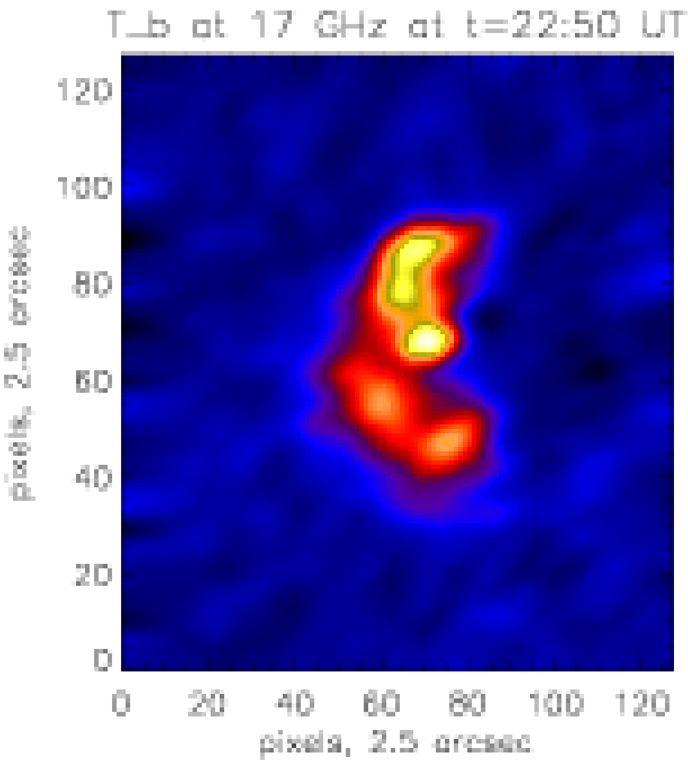

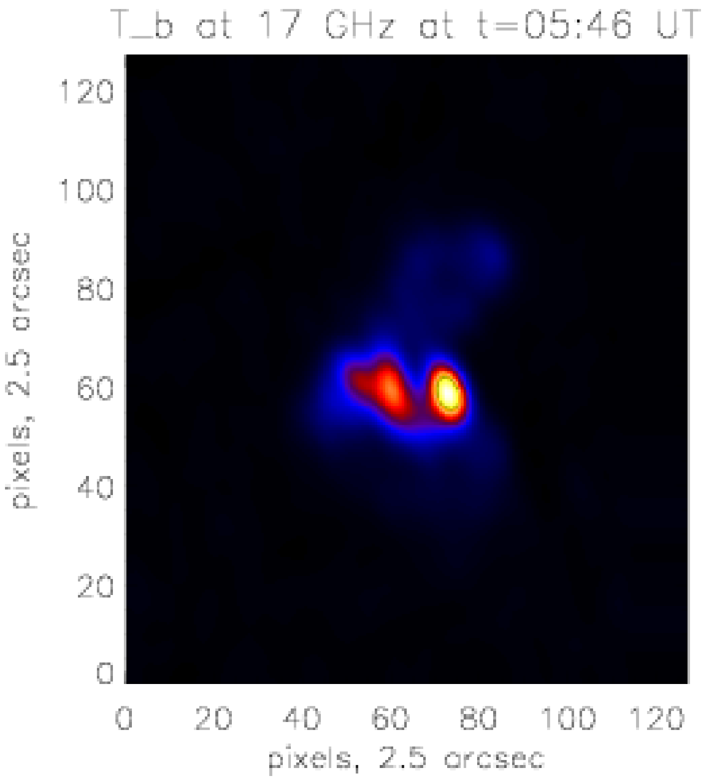

22:50 UT → 05:46 UT

During 6.5 hours before the start of the M1.2 flare, the spatial distribution of radio brightness changed dramatically: from two almost parallel loop-like structures elongated in the north-south direction with positive polarizations of southern bases and negative polarizations of northern bases at the beginning of observations (22:50 UT) before the appearance of a bright loop-like structure elongated in the east-west direction, ~ 2.5 hours before the start of the flare. This transverse structure continued to grow stronger and became a source of relatively powerful microwave emission from the flare.

Fine spatial structure of sources

Ignition of a system of EUV intersecting loops (X-structure), simultaneous with the appearance of a strong nonstationarity of radiation from microwave sources 1, 3, and 4.

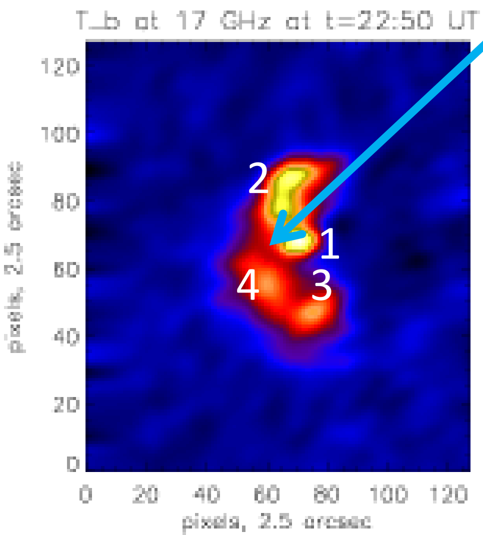

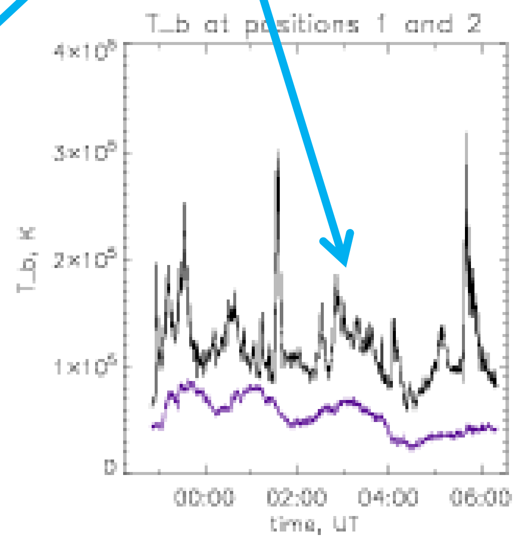

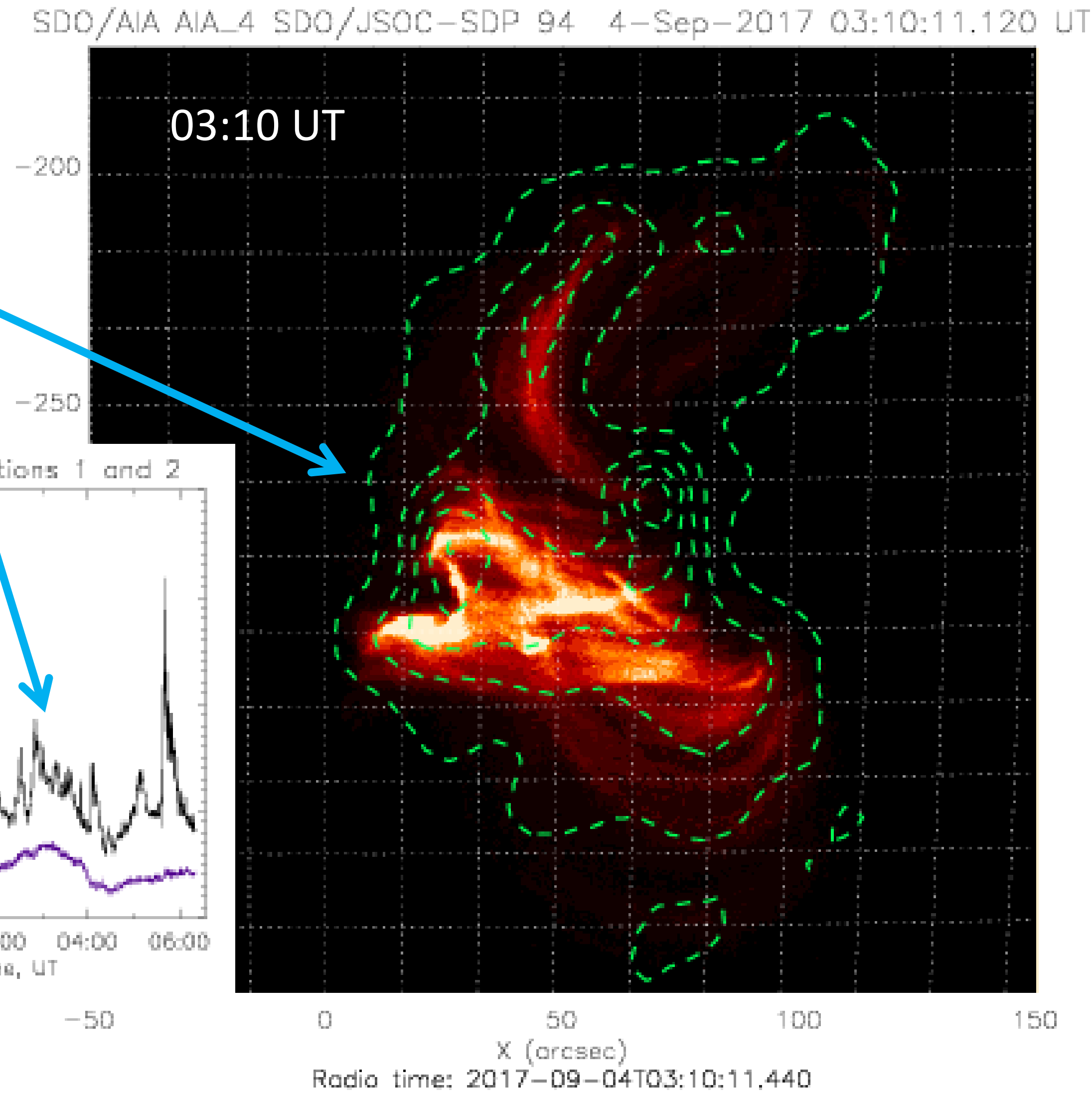

Mutual arrangement of EUV, radio sources and magnetic field islands

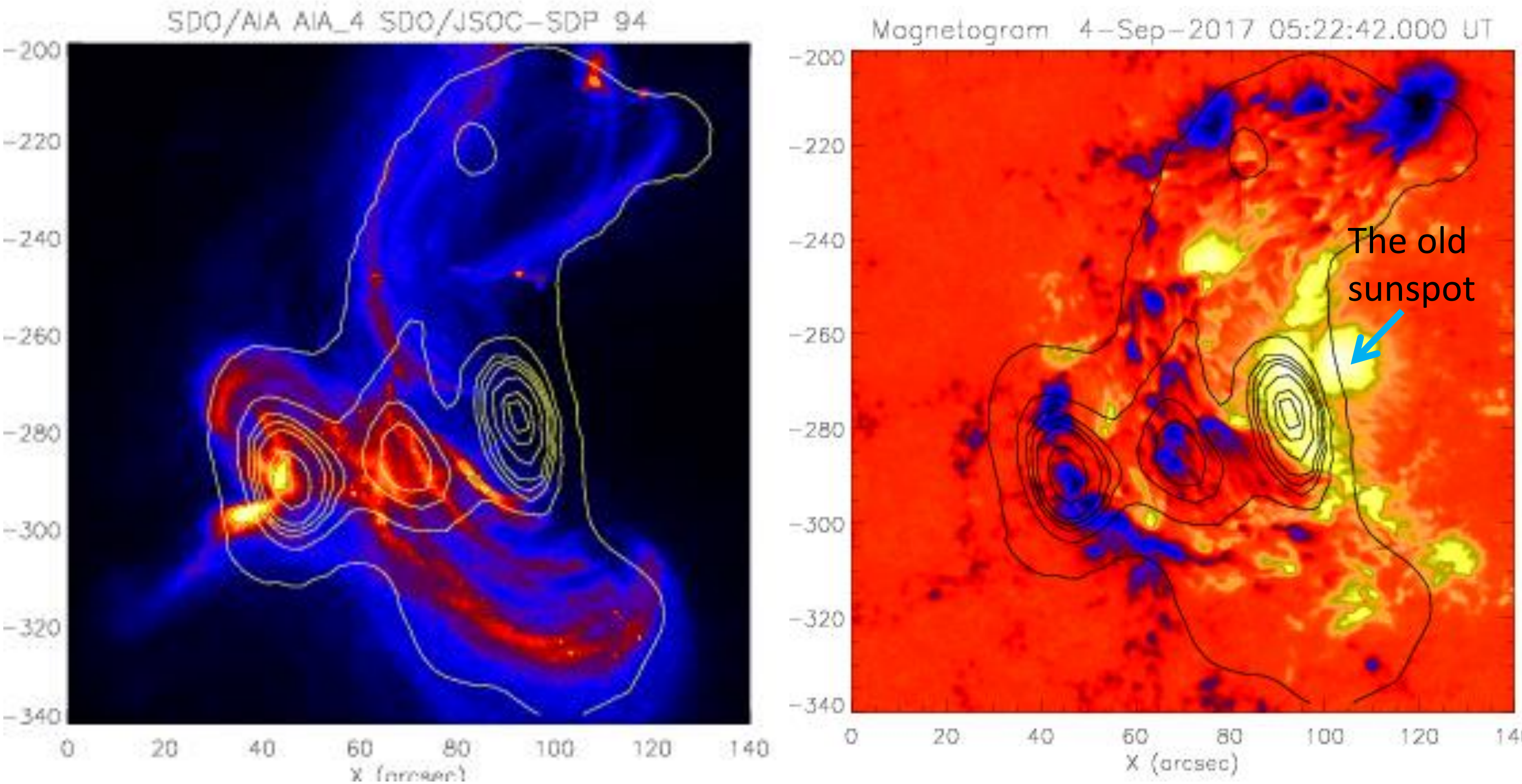

From the joint analysis of EUV (brightness) and radio (contours) emission maps with magnetic field maps, it is clear that bright EUV loops and microwave sources arise in the region of the emergence of NEW magnetic fluxes. There is no bright nonstationary emission in the OLD sunspot.

An analysis of the five events studied in this work without CME (“confined”) shows a character of the development of preflare dynamics similar to the one mentioned above in our previous works.

In the event 30-07-2011 (NOAA 11261), crossing EUV loops appear ~ 3 hours before the onset of the flare in the southern part of AR (Fig. 1). The center of the radio emission in intensity falls on the crosshair of the X-structure in the EUV (Fig. 1a). Before the flare, the radio source has a vertical (oriented in the North-South direction) structure (Fig. 1 c).

During and after the flare, the structure is almost horizontal (Fig. 1d). A flare radio source at 17 GHz is initiated in the place where from the very beginning of observations at NoRH (22:50 UT), small (~ 10 ″) X-structures in the EUV were visible (Fig. 1 a). Moreover, the most dynamic, active group of EUV loops is also the region of the brightest radio emission. This is also where the flare of M occured.

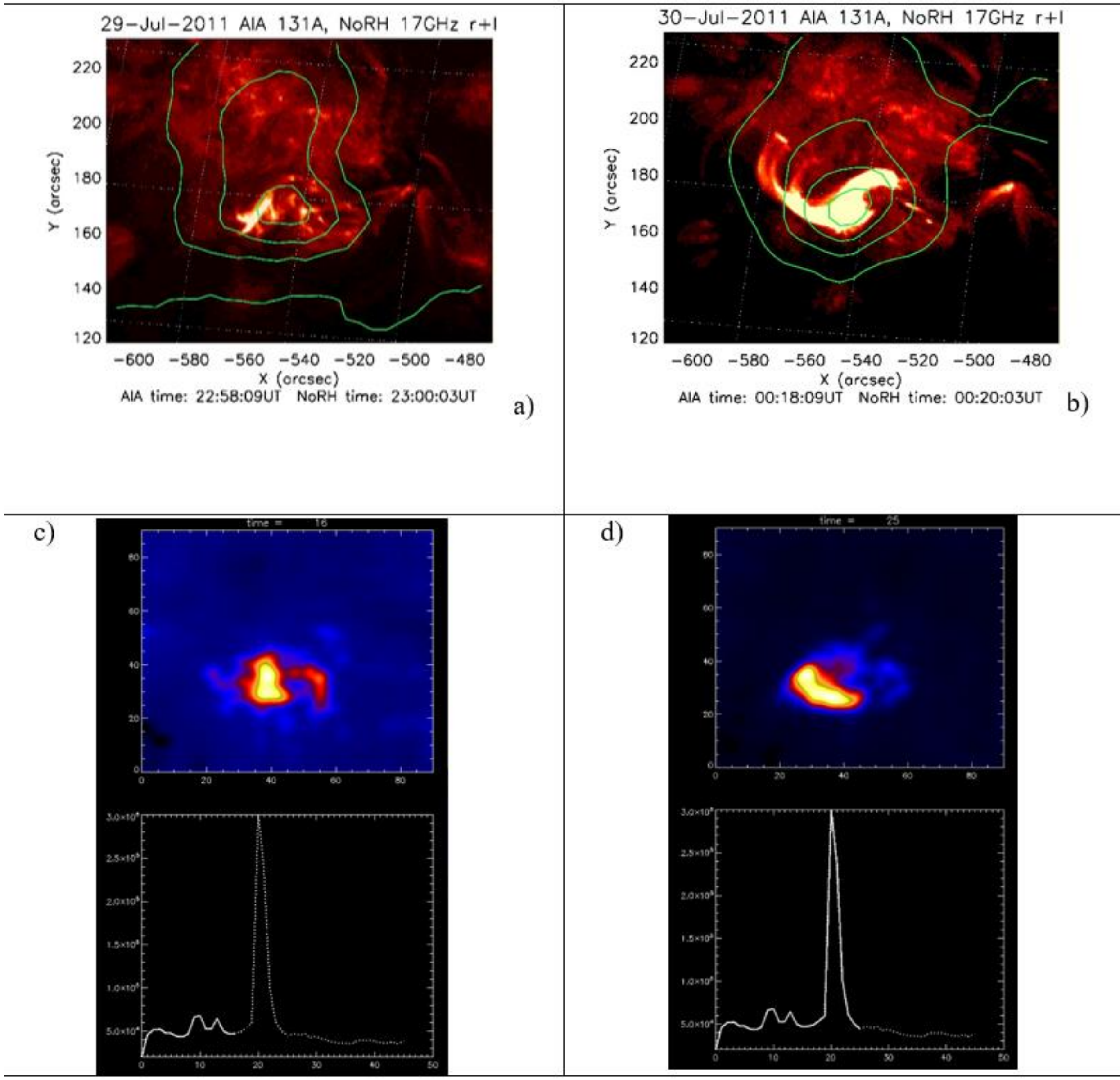

Fig. 1 a) and b) - superposition of two-dimensional images in the intensity of radio emission (Stokes parameter I) (contours) at a frequency of 17 GHz on the EUV 131 Å SDO / AIA map for NOAA 11261 on July 30, 2011; c) and d) - two-dimensional images in the intensity of radio emission (Stokes parameter I) and time profiles from the region of the radio source with coordinates (40.30), where the maximum radio brightness was observed in NOAA 11261 on July 30, 2011. The light line on the time profile shows the moment of observation of the two-dimensional radio brightness. In Figures c and d, bottom panel: vertical axis - brightness temperature, K, horizontal axis - time point in counts from the beginning of observations NoRH (22:50 UT).

Рис. 1.

Fig. 2 shows the spatial and temporal dynamics in the 2011-10-02 event (NOAA 11305). Here, an hour before the M flare (at 00:08:09 UT), a bright EUV loop with a size of ~ 50 ″ appears, which exactly coincides with the loop in the radio emission (Fig. 2a). At 00:14 UT, before the start of the M-class flare, the horizontal EUV loop split into intersecting structures with a maximum radio emission above the forks (crosshairs) of the loops. A new, transverse structure is formed during the flare itself (00:38 UT) (Fig. 2b). Moreover, the maximum of radio emission is shifted during the flare from the base of this transverse structure to its apex (00:41 UT). The appearance of the radio brightness maximum at the top of the loop is a fairly frequent phenomenon observed in individual flare loops (Melnikov et al. 2002). In this event, we did not observe small X-structures in the EUV, mainly large arches with a size of ~ 40 ″, at first - horizontal, then, during the M flare itself, vertical, after the flare - again horizontal.

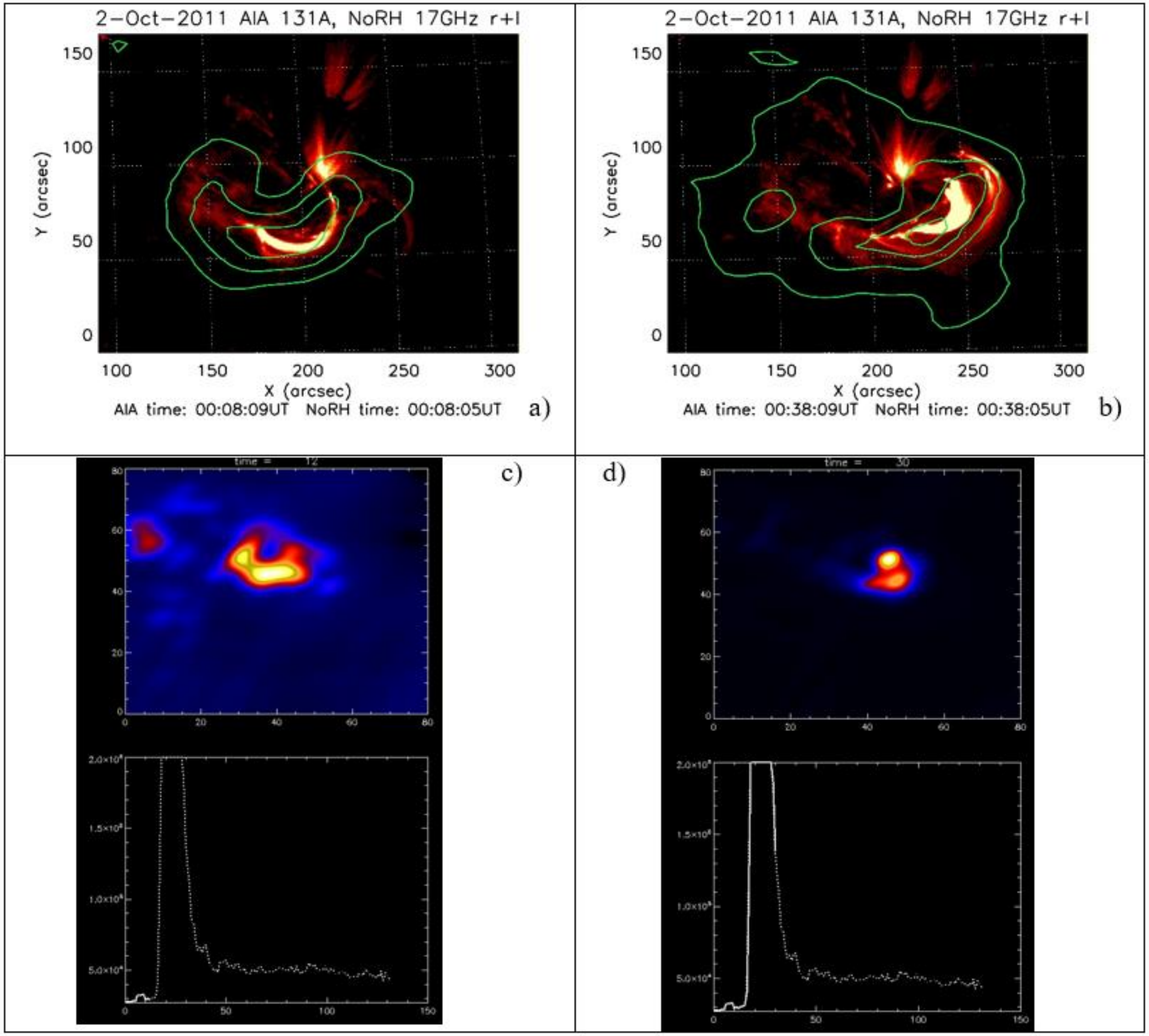

Fig. 2
The same as Fig. 1 for the October 2, 2011 event, NOAA 11305.

Рис. 2.

Fig. 3 shows the spatial dynamics in the event 2012-10-05 (NOAA 11476). Before the M5.7 flare (04:11 UT), three C-class flares occur sequentially in different parts of the AR. The first crossed EUV loops are observed at 00:36 UT, 3.5 hours before the M flare. One can see a strong thermal cyclotron source ("radio spot"), around which a lot of small-size EUV arches are shining. The 17 GHz burst radio source originates northeast of the main radio spot. Immediately before the flare (04: 04UT), small X-structures 10 ″ –15 ″ in the EUV appear (Fig. 3 a and b). And here, similarly to the previous cases, a radio source appears in the crosshairs of the EUV arches. During the flare (04: 28UT), huge closed structures in the EUV are visible (Fig. 3 c and d). It is noteworthy, therefore, that the emerging radio source is projected again exactly onto the small X-structures in the EUV, where the M flare is initiated.

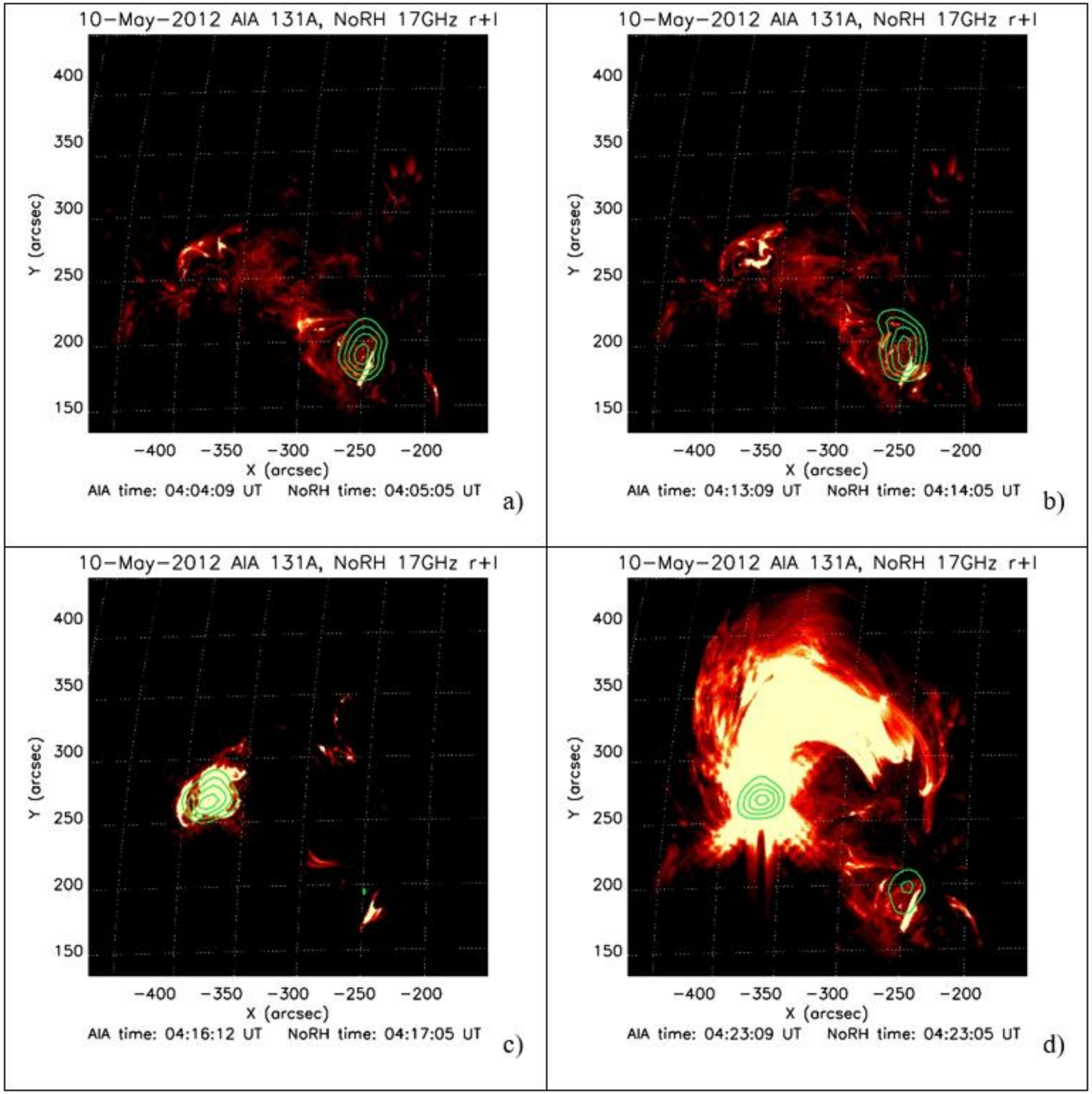

Fig. 3 a), b), c), d) - superposition of two-dimensional images in the intensity of radio emission (Stokes parameter I, contours) at a frequency of 17 GHz on the EUV 131Å SDO / AIA map for NOAA 11476 on May 10, 2012.

Рис. 3.

In the non-eruptive NOAA 11884 2013-03-11, X-structures are visible from the very beginning of observations at NoRH (22:50 UT) (Fig. 4 a), and the M-class flare itself occurs closer to the end of observations, at 05:16 UT. The radio source above these structures is unstable, it appears and disappears during the time of observations (from 01:40 to 04:15 UT, it is not observed at all). During the flare, which begins at 05:15 UT in radio emission, we see a radio source at the same place where, five hours before the flare, at the beginning of observations, small (10 "-15") X-structures appeared. The flare is again initiated exactly here, and the maximum of radio emission in intensity at the moment of the onset of the flare is projected just on the "crosshair" (Fig. 4 b).

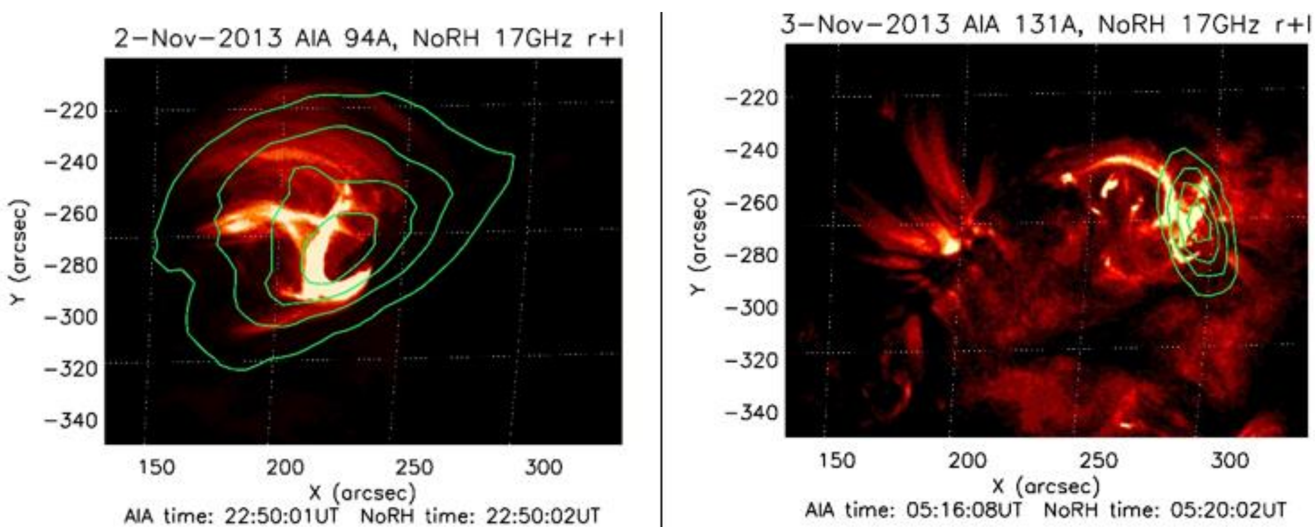

Fig. 4

a)

b)

In the event 2014-02-04 (NOAA 11967), an hour before the M flare (at 00:41 UT), two crossed systems of large loops (~ 40 ″) and four radio sources appear. The third one from the left appears at the top of the EUV loop; it is brighter than to the left located polarized cyclotron sources. The fourth radio source appears in a transverse loop (Fig. 4 c and d). Moreover, the flare process takes place exactly at the location of the third and fourth radio sources.

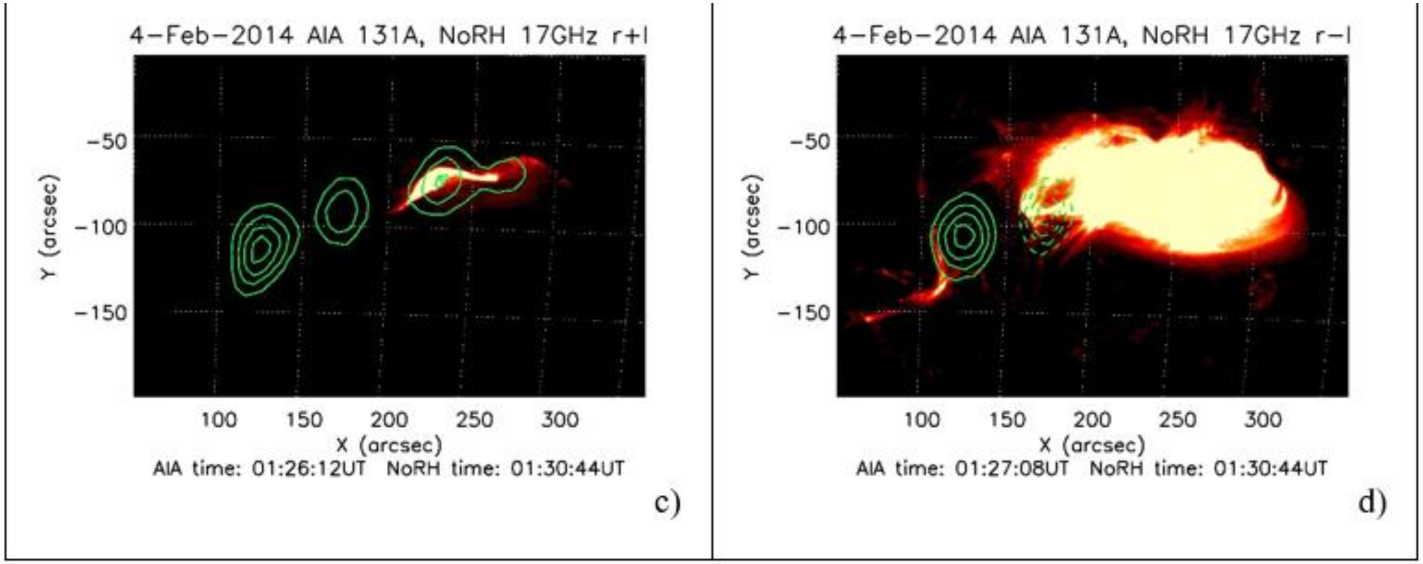

Fig. 4

Thus, events without CMEs in most of the ARs studied are characterized by the appearance of X-structures in the EUV emission several hours or immediately before the M-class flare.

An M-class flare is subsequently initiated in the area where the X-structures are located.

In a number of events, transverse structures appear in the radio emission before the flares of M. In our sample of 5 non-eruptive events, during the flares themselves, the maximum of the radio emission falls on the top of the transverse structures in the EUV.

Radio sources associated with flares, in the pre-flare phase, demonstrate instability, they may appear and disappear, and then become brightly manifested themselves during the flare.

As in our previous studies (Bakunina and Melnikov, 2019; Bakunina et al., 2020 a; Bakunina et al., 2020 b), it was revealed that the region of strong nonstationarity often falls within the intersunspot zone with a low degree of polarization (radio sources in the “crosshair ").

Study of spatial and temporal dynamics for events with CME

Note that, for all five "confined" events, the flare areas are small compared to events with CME. These are usually compact, limited flares. The areas of radio sources, according to table. 1, also demonstrate lower values (<23000 arcsec^2), in contrast to events with CME, where the areas of radio sources are noticeably larger (> 30000 arcsec^2).

A characteristic feature of the active regions that produced CME is not only the larger size of the radio source and the area of the flare itself, but also the presence of a polarized radio source during several hours before flare in the place where the flare will occur.

Fig. 5a shows an example of the existence of a polarized source 1.5 hours before the onset of the M flare in the region of rather large X-structures (in the figure - on the right). In Fig. 5b, the same source (on the right) in intensity (Stokes parameter I) 30 minutes before the onset of the flare is located in the region of already strongly luminous EUV loops at a wavelength of 94 Å. Figures 5c and 5d show the view of the radio source on 17 GHz intensity maps: in Fig. 5 c - immediately before the flare and in Fig. 5 d - in its active phase after the peak. We see that the burst in radio emission occurs exactly in the place where the polarized radio source was located above the X-structures. This AR (NOAA 11283) in the sample of six events is the only one not closely adjacent to other ARs.

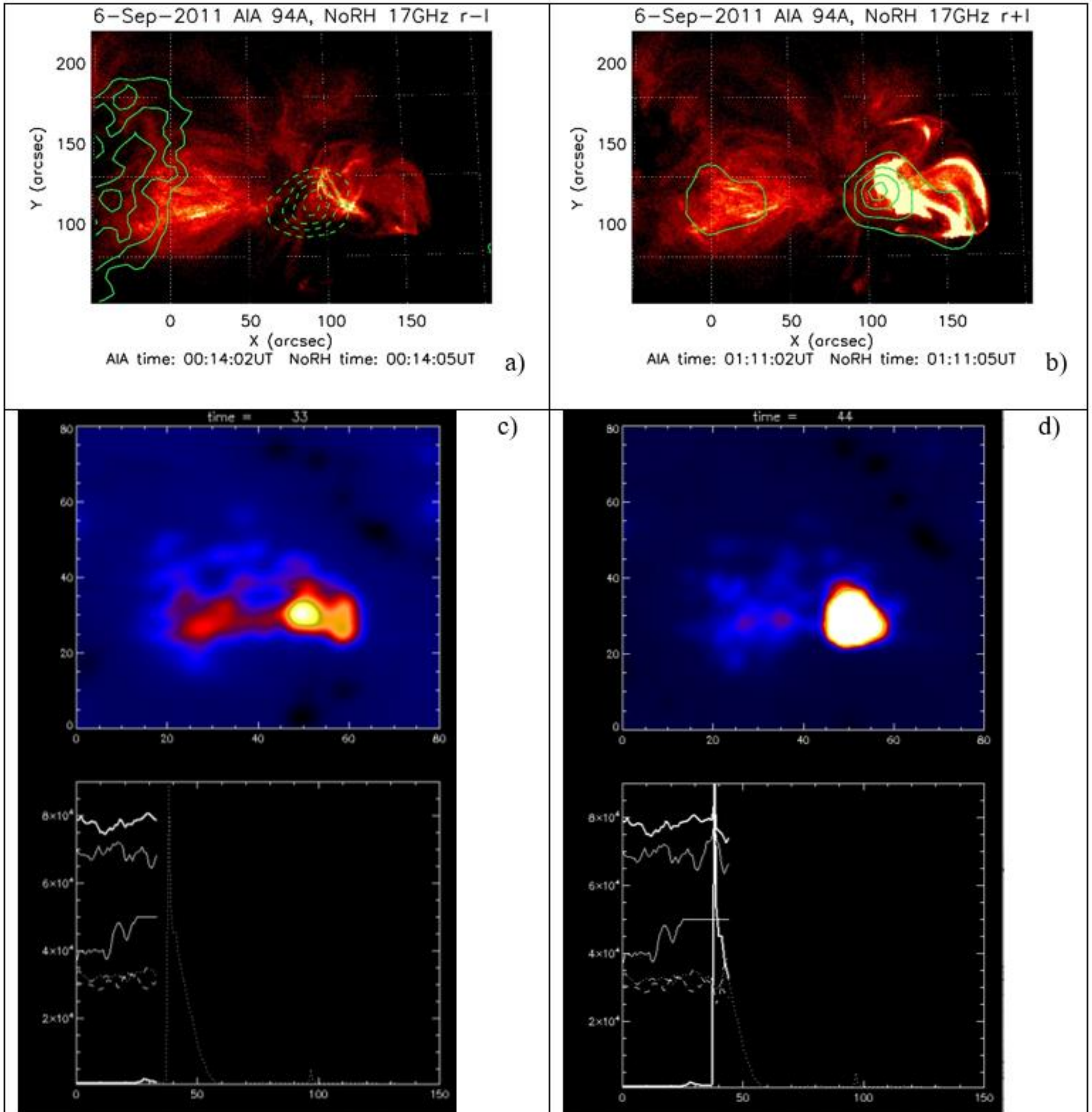

Fig. 5 a), b) - superposition of two-dimensional images in the intensity of radio emission (Stokes parameter V, contours) at a frequency of 17 GHz on the EUV 131Å SDO / AIA map a) and b) - Stokes parameter I, contours. c) and d) - two-dimensional images in the intensity of radio emission (Stokes parameter I) and time profiles from the region of the radio source with coordinates (52, 28), where the maximum radio brightness was observed in NOAA 11283 on September 6, 2011. (for an eruptive flare). The light line on the time profile shows the moment of observation of the two-dimensional radio brightness. Other time profiles show pre-flare oscillations from different parts of the AR. In Figures c and d, bottom panel: vertical axis - brightness temperature, K, horizontal axis - time point in counts from the beginning of observations NoRH (22:50 UT).

Рис. 5

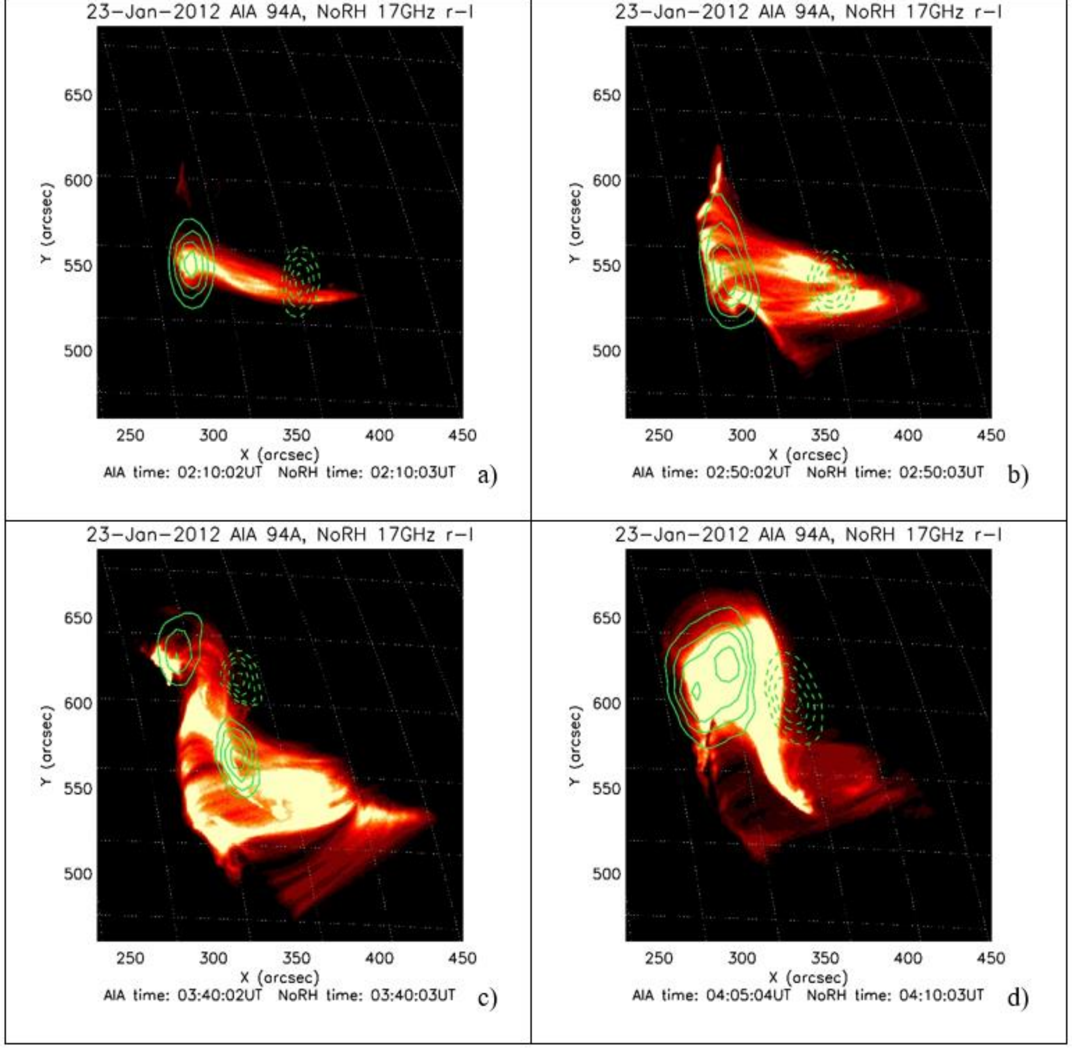

Fig. 6 a), b) - superposition of two-dimensional images in circular polarization of radio emission (Stokes parameter V, contours) at a frequency of 17 GHz on the EUV 94 Å SDO / AIA card before the flash and c) - before the peak of the flash, d) - after the peak of flare at NOAA 11402 on 23 January 2012

If in the previous event we did not observe transverse structures in the radio emission before and during the flare, then in NOAA 11402 on January 23, 2012, huge sizes of loops, up to 100 ″ long, and the appearance of new, transverse loops (arcades) before the flare are observed (Fig. 6). The transverse structure in the radio emission can be seen 170 minutes before the start of the M-class flare. Here we observe the rotation of the flare radio source, which means the emergence of a shear angle and the restructuring of the magnetic field during the flare.

This flare has a record duration in our sample of events with a slow rise, impulse phase, and slow decline, stretching for 4.5 hours. The transverse structure in the EUV is clearly visible, with microwave emission well correlated with it before the peak phase of the flare and immediately after it (Fig. 6 c, d). Here we do not see small, compact EUV loops.

The other three ARs from the sample of events with CME - NOAA 11877 (October 24, 2013), NOAA 12173 (September 28, 2014), and NOAA 12242 (December 17, 2014), also demonstrate the existence of a polarized radio source in the region of crossed EUV loops, where the flare is subsequently initiated.

Fig. 7 shows how the CME flare in NOAA 11429 on March 9, 2012 was triggered by the intersection of a small EUF loop with a long loop. First, we see a horizontal structure with a maximum of radio emission at the intersection of the small and long EUV loops (Fig. 7a). At the peak of the flare, a transverse structure in the radio emission and brightly luminous sigmoid loops in the EUV on the neutral line are clearly visible (Fig. 7 d).

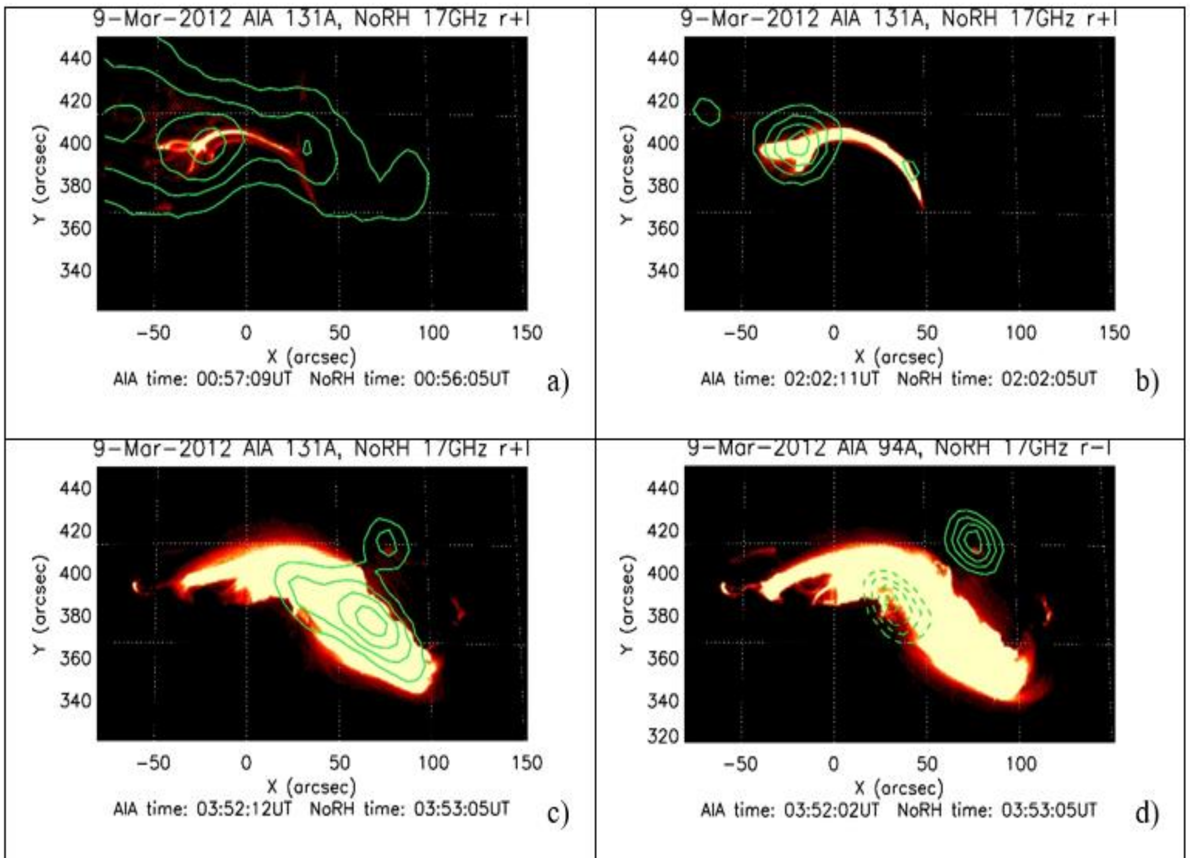

Fig. 7 a), b), c) - overlay of two-dimensional images in intensity (Stokes parameter I, contours) and d) - in circular polarization of radio emission (Stokes parameter V, contours) at a frequency of 17 GHz on a map of EUV radiation of 131 Å SDO / AIA before flash - Figures a) and b). Figure c) (131 Å), figure d) (94 Å) - at the maximum of the flare in NOAA 11429 on March 9, 2012. The transverse structure in radio emission and bright EUV sigmoid loops on the neutral line are clearly visible.

The study of magnetograms of the complete solar disk showed that the AR, in which an event with CME occurs, as a rule, is closely adjacent to another AR (five cases out of six). At SDO / AIA, at different wavelengths, either giant loops connecting both ARs or open lines of force in the space between two ARs are observed.

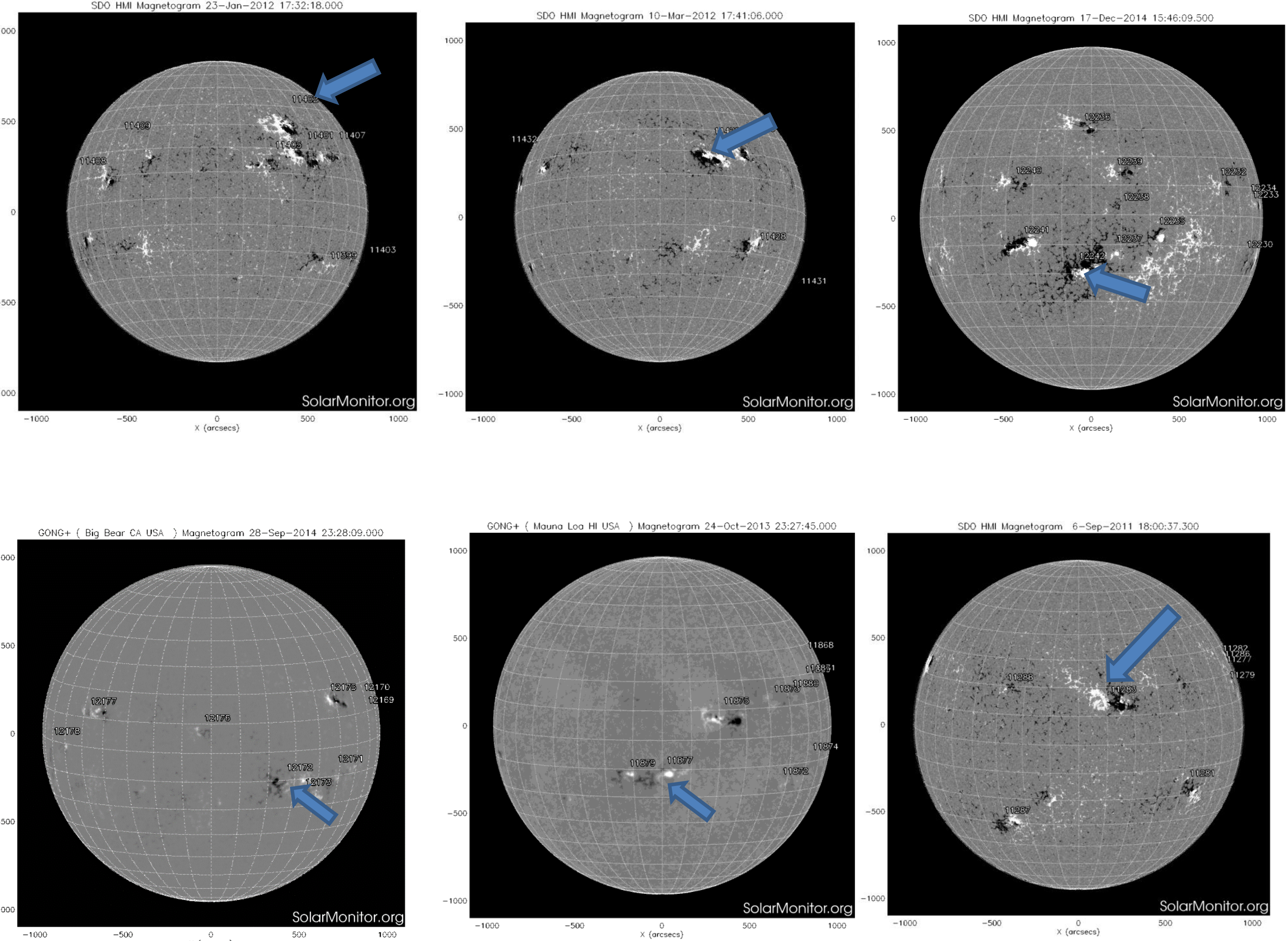

SDO HMI Magnetogram 23-Jan-2012 17:32:18.000
11402
11409
11401
11407
11405
11408
11399
11403
SolarMonitor.org
X (arcsecs)
SDO HMI Magnetogram 10-Mar-2012 17:41:06.000
11432
11428
11431
SolarMonitor.org
X (arcsecs)
SDO HMI Magnetogram 17-Dec-2014 15:46:09.500
12236
12239
12240
12232
12234
12233
12238
12235
12241
12237
12230
12242
SolarMonitor.org
X (arcsecs)
GONG+ (Big Bear CA USA) Magnetogram 28-Sep-2014 23:28:09.000
12175
12170
12169
12177
12176
12178
12171
12172
12173
SolarMonitor.org
X (arcsecs)
GONG+ (Mauna Loa HI USA) Magnetogram 24-Oct-2013 23:27:45.000
11868
11875
11874
11879
11877
11872
SolarMonitor.org
X (arcsecs)
SDO HMI Magnetogram 6-Sep-2011 18:00:37.300
11282
11286
11277
11279
11288
11283
11281
11287
SolarMonitor.org
X (arcsecs)

Analysis of the integrated microwave spectra obtained from observations with the RATAN-600 showed that the dynamics of the frequency spectrum of microwave emission may differ before different types of flares - eruptive and non-eruptive. As an illustration, Fig. 8 shows the frequency spectra observed before four flares: two eruptive (NOAA 11283 and 12242) and two non-eruptive (NOAA 11261 and 11305). In the case of eruptive events on the day of the flare and, most likely, the day before, an increase in the slope of the spectrum in the short-wavelength part is observed. Perhaps this is due to the development of an NLS source (an intersunspot source above the neutral line of the magnetic field). In the case of non-eruptive events, the slope of the spectrum in the short-wavelength part either does not change or increases significantly less than for eruptive events.

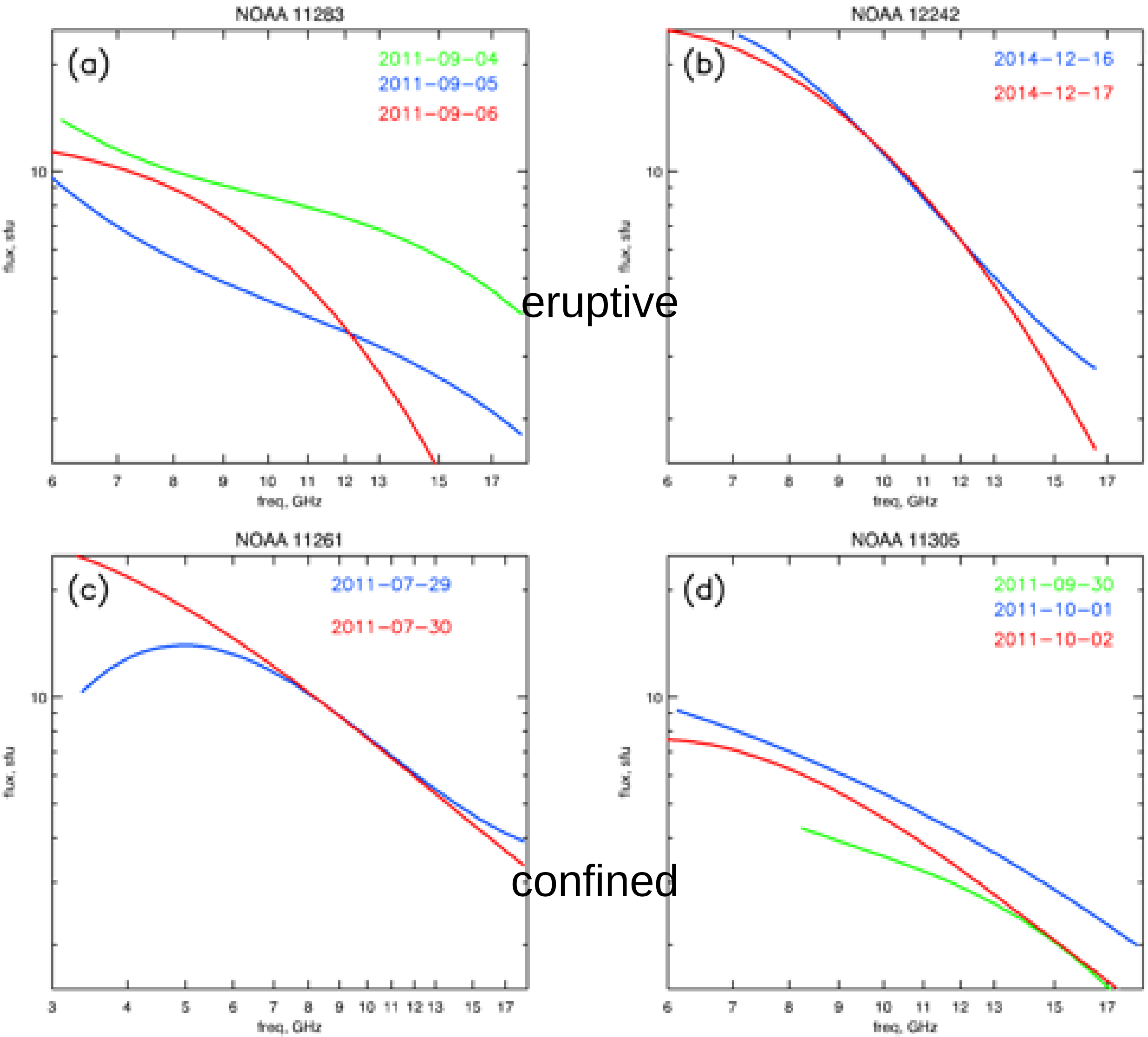

Fig.8

Difference in the dynamics of the frequency spectrum of microwave radiation before different types of flares - eruptive: a) for NOAA 11283 and b) for NOAA 12242 and non-eruptive: c) for NOAA 11261 and d) for NOAA 11305. The day of the event under study is marked in red, blue and green - the previous two days.

Conclusions:

Both for ARs with flares of the "confined" type, and for ARs with CME, it is typical:

1. The appearance of X-structures in the EUV radiation a few hours or immediately before the M-class flare. These structures are associated with radio emission at 17 GHz, the maximum of which falls on the “crosshair” of the EUV loops.

2. An M-class flare is subsequently initiated in the area where the X-structures are located.

3. In a number of events, transverse structures appear in the radio emission before the flares of M.

Features of non-eruptive M-class flares:

1. During flares of the X-ray class M, the maximum of radio emission falls on the top of the transverse EUV structures.
2. Radio sources associated with flares, in the preflare phase, demonstrate instability, can appear and disappear, and then become brightly manifested during the flare itself.
3. In three events out of five, small magnetic arches are clearly visible, their size is only ~ 10 arcsec (~ 7000 km). Perhaps this speaks of a compact, low and therefore strong magnetic field, which is difficult to break apart by the moving masses of the plasma, and, therefore, we observe the type of event "confined".
4. The region of strong nonstationarity often falls on the intersunspot zone with a low degree of polarization (radio sources in the "crosshair"). The same region is the region of the brightest radio emission, where the M-class flare subsequently occurs. Perhaps, it is in this region that a lot of free magnetic energy accumulates, and besides, it is there that the magnetic structures are most unstable. It is thanks to these two factors that an M-class flare is initiated in this location.

For events with CME, or eruptive, we found some differences from “confined” events:

1. Events with CME demonstrate more extensive radio sources in area, which may be explained by the glow of more extended magnetic arcades.
2. The study of magnetograms of the complete solar disk showed that the AR, in which the event with CME occurs, as a rule, is closely adjacent to another AR (five cases out of six). At SDO / AIA, at different wavelengths, either giant loops connecting both ARs or open lines of force in the space between two ARs are observed.
3. In the pre-flare phase in eruptive ARs, polarized radio sources are stably observed in the region of X-structures in EUV radiation, and these X-structures are most often large in size (up to 100 ″), where a flare is subsequently initiated.
4. There are noticeable differences in the spectra of eruptive and non-eruptive ARs: for ARs with CME, changes in the spectrum in the short-wavelength part during one or two days before the flare are more significant.

Literature

Bakunina I.A., Melnikov V.F. Dynamics of solar microwave emission before powerful flares in September 2017. A&AT. V. 31. Issue 3. P. 251-266. 2019.

Bakunina I.A., Melnikov V.F., Morgachev A.S. Preflare Dynamics of Microwave and Ultraviolet Emission in Active Regions of the Sun. Astrophysics. V. 63. Issue 2. P. 252-259. 2020 a.

Bakunina I. A., Melnikov V., Morgachev A. S. Signs of Preflare Situation in Solar Ultraviolet and Microwave Emission. Geomagnetism and Aeronomy. Vol. 60. No. 7. P. 853-859, 2020 b

Duan A., Jiang C., He W., Feng X., Zou P., Cui J., A Study of Pre-flare Solar Coronal Magnetic Fields: Magnetic Flux Ropes. ApJ. V. 884. Article id. 73. 16 pp. 2019.

Melnikov V.F., Shibasaki K., Reznikova V.E. Loop-top nonthermal microwave source in extende flaring loops. ApJ. V. 580. L185-L188. 2002.

Sharykin I.N., Zimovets I.V., Myshyakov I.I. Flare Energy Release at the Magnetic Field Polarity Inversion Line during the M1.2 Solar Flare of 2015 March 15. II. Investigation of Photospheric Electric Current and Magnetic Field Variations Using HMI 135 s Vector Magnetograms. ApJ. V. 893. Article id. 159. 25 pp. 2020.